HETEROCYCLES, Vol. 104, No. 8, 2022, pp. -. © 2022 The Japan Institute of Heterocyclic Chemistry
Received, 27th April, 2022, Accepted, 10th June, 2022, Published online, 21st June, 2022
DOI: 10.3987/COM-22-14679

CHEMICAL STRUCTURES AND CELL DEATH INDUCING ACTIVITIES OF CONSTITUENTS ISOLATED FROM *HIBISCUS TILIACEUS*

Takahiro Kitagawa, Takahiro Matsumoto,* Daisuke Imahori, and Tetsushi Watanabe*

Department of Public Health, Kyoto Pharmaceutical University, Misasagi, Yamashina-Ku, Kyoto 607-8412, Japan; E-mail: tmatsumo@mb.kyoto-phu.ac.jp (T.M.), watanabe@mb.kyoto-phu.ac.jp (T.W.)

Abstract – A new coumarin glycoside hibiscuscoumarin (**1**) was obtained with ten known compounds including seguinoside K (**7**) from the stems and twigs of *Hibiscus tiliaceus*. The structure of hibiscuscoumarin (**1**) was elucidated based on the chemical/physicochemical evidence. The cell death-inducing activities of the isolated compounds with or without Adriamycin (ADR) were observed using time-lapse cell imaging. The isolated compounds did not affect the number of mitotic entry cells and dead cells. Otherwise, the treatment of cells with seguinoside K (**7**) significantly increased the number of dead cells induced by ADR.

The plant *Hibiscus tiliaceus* (Malvaceae) grows widely in the littoral forests and mangrove forest margins in tropical and subtropical regions.[1] It is used as a traditional medicine for the treatment of diarrhea, dysentery, and typhoid.[2] The extract of this plant has several bioactivities; anti-inflammatory,[3] antioxidant,[4] and tyrosinase inhibitory activities.[5] In our ongoing research to discover new cancer treatment and prevention agents, we reported about elemophilane-type sesquiterpenoids, pyrone derivatives, and pyrrole alkaloids as inhibitors of cancer stem cell proliferation, Wnt/β-catenin signaling, and P-glycoprotein (P-gp) activity.[6–8] In the course of these studies, we recently reported the chemical structures of several isolated compounds from the methanolic extract of the stems and twigs of *H. tiliaceus* and their cytotoxic activities against HeLa cells.[9] As a continuing study, we obtained eleven compounds including a new coumarin glycoside hibiscuscoumarin (**1**), from the stems and twigs of *H. tiliaceus*. The combinational effects of isolated compounds (**1**–**11**) with ADR on HeLa cells were evaluated by time-lapse imaging analysis.

Adriamycin (ADR) is a chemotherapeutic drug used for the treatment of several cancers.[10] ADR interacts with DNA via intercalation between the base pairs of the duplex DNA, inducing cell death. However, the clinical utility of ADR is limited due to side effects such as cardiotoxicity.[11] Therefore, compounds enhancing the cytotoxicity of ADR on cancer cells can reduce the dosage of ADR, thereby avoiding the side effects.

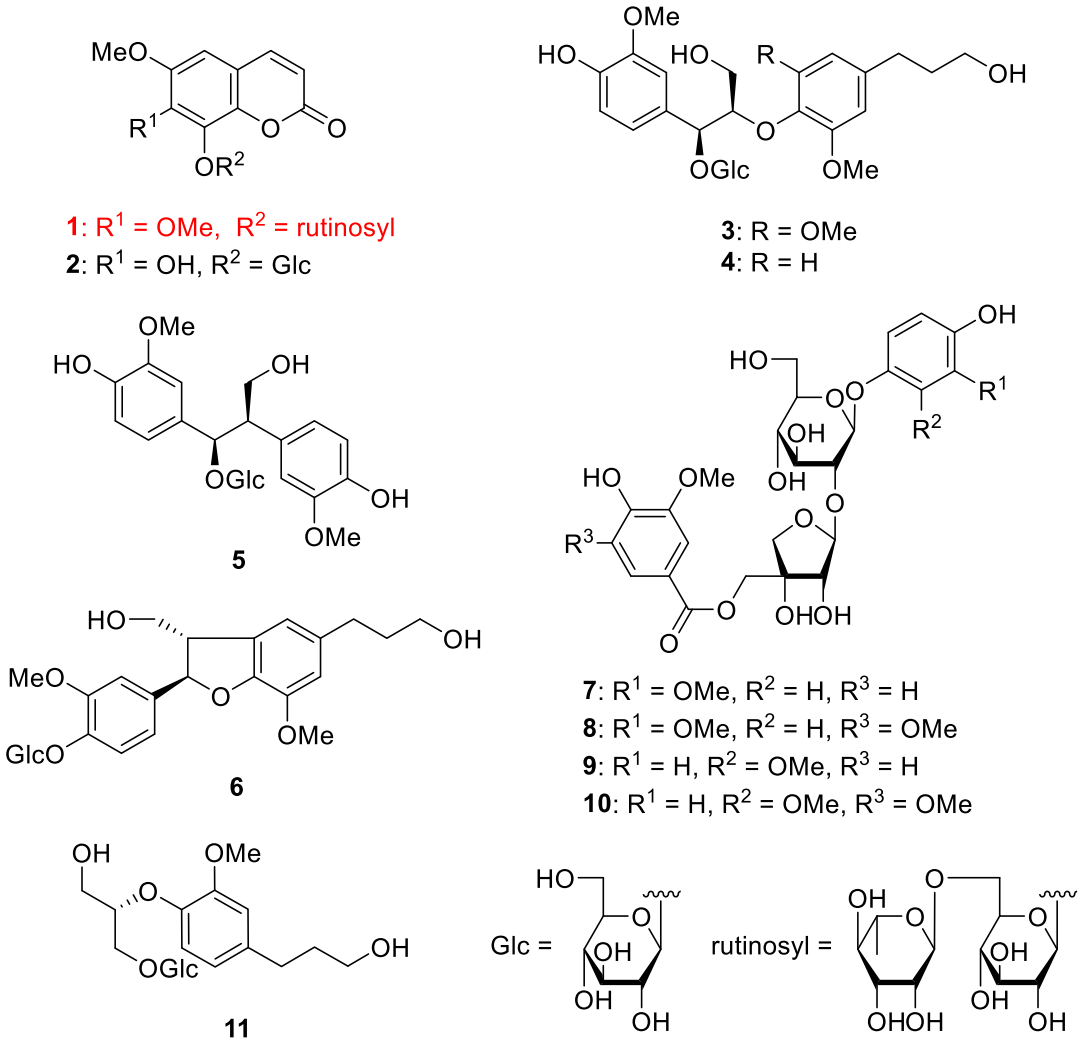

Figure 1. The chemical structures of the isolated compounds from the stems and twigs of *H. tiliaceus*

The methanolic extract of the fresh stems and twigs of *H. tiliaceus* was partitioned in ethyl acetate–water (1:1, v/v) to furnish an ethyl acetate soluble fraction and aqueous layer. The aqueous layer was further extracted with *n*-butanol to give *n*-butanol (0.20%) and water (1.14%) soluble fractions. The *n*-butanol soluble fraction was subjected to normal- and reversed-phase silica gel column chromatography and repeated high-performance liquid chromatography (HPLC) to give a new compound, hibiscuscoumarin (**1**, 0.000013%), and ten known compounds; fraxin (**2**, 0.000047%),[12] rourinoside (**3**, 0.000017%),[13]

7*S*,8*S*-4,9,9'-trihydroxy-3,3'-dimethoxy-8-*O*-4'-neolignan-7-*O*-*β*-D-glucopyranoside (**4**, 0.000033%),[14] hovetrichoside A (**5**, 0.000049%),[15] dihydrodehydrodiconiferyl alcohol-4-*O*-*β*-D-glucopyranoside (**6**, 0.000012%),[16] seguinoside K (**7**, 0.000067%),[17] albibrissinoside B (**8**, 0.000033%),[18] millettiaspecosides A (**9**, 0.000018%),[19] millettiaspecosides B (**10**, 0.000012%),[19] and 2-[4-(3-hydroxypropyl)-2-methoxyphenoxy]-1,3-propanediol 1-*O*-glucoside (**11**, 0.000017%).[20]

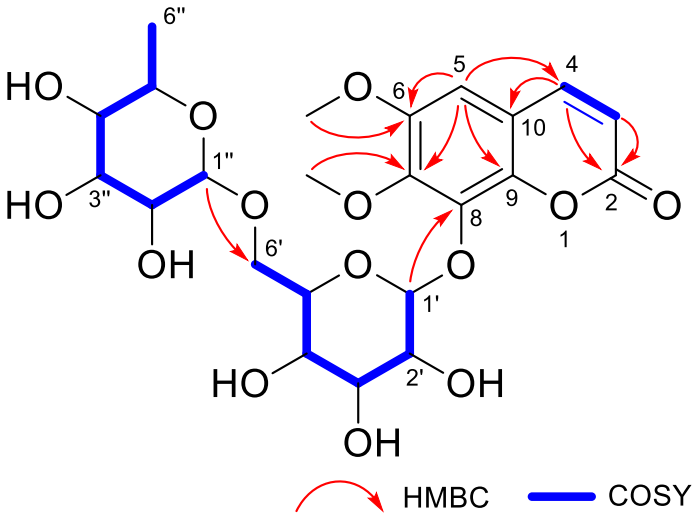

Figure 2. The important 2D-NMR correlations of hibiscuscoumarin (**1**)

Hibiscuscoumarin (**1**) was obtained as a colorless amorphous powder with negative optical rotation ([α]$^{25}_{D}$ -65.7, MeOH). The molecular formula ($C_{23}H_{30}O_{14}$) was determined via high-resolution electrospray-ionization mass spectrometry (HRESIMS) and ^{13}C-NMR spectroscopy. The ^{1}H- and ^{13}C-NMR spectra (CD_3OD) of **1** (Table 1) showed characteristic signals of 6,7,8-trisubstituted coumarin {*cis*-olefinic proton signals [δ_H 6.25 (d, J = 9.2, H-3) and 7.79 (d, J = 9.2, H-4)], an aromatic proton signals [6.93 (s, H-5)], two methoxy groups [δ_H 3.81 (s, H-6-OMe) and 3.87 (s, H-7-OMe)], an ester carbonyl group [δc 163.0 (C-2)]}, glucose moiety, and rhamnose moiety. The positions of each functional group were determined by COSY double quantum filter (DQF COSY) and heteronuclear multiple bond correlation (HMBC) spectra shown in Figure 2. The HMBC correlations of H-6-OMe/C-6, H-7-OMe/C-7, H-1'/C-8, and H-1"/C-6' suggested that the methoxy groups were located at C-6 and C-7 positions, and the glucose and rhamnose moieties were attached to the C-8 and C-6' positions. Acid hydrolysis of **1** with 5% aqueous H_2SO_4−1,4-dioxane yielded D-glucose and L-rhamnose. These sugars were identified via HPLC by the chiral tolylthiocarbamoyl-thiazolidine derivatives of them as described previously.[21] Based on the evidence, the chemical structure of hibiscuscoumarin (**1**) was established as shown in Figure 1.

Table 1. ^{13}C- (150 MHz) and ^{1}H- (600 MHz) NMR data of hibiscuscoumarin (**1**) in CD_3OD

position	δ_C	δ_H (J in Hz)
2	163.0	
3	115.5	6.26 (d, 9.6)
4	146.1	7.80 (d, 9.6)
5	106.4	6.93 (s)
6	151.8	
7	147.3	
8	138.0	
9	143.9	
10	116.1	
6-OMe	56.8	3.81 (s)
7-OMe	62.1	3.87 (s)
1'	104.2	5.08 (d, 8.4)
2'	75.7	3.43 (m)
3'	77.2	3.25 (m)
4'	72.2	3.46 (m)
5'	77.9	3.35 (m)
6'	68.0	3.41 (m) 3.77 (m)
1"	102.3	4.41 (d, 1.6)
2"	72.1	3.35 (m)
3"	71.7	3.23 (m)
4"	73.9	3.17 (m)
5"	69.7	3.25 (m)
6"	17.9	1.00 (d, 6.0)

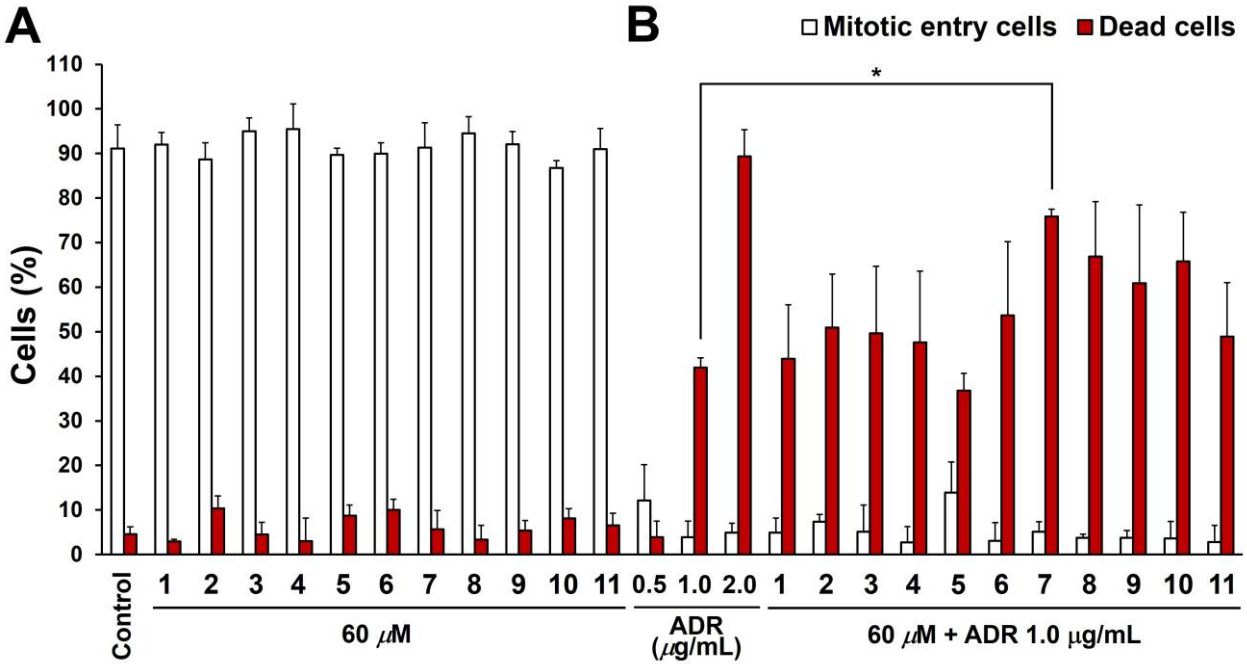

Figure 3. The effects of isolated compounds (**1**–**11**) and ADR on cell proliferation and cell death. (A) HeLa cells were treated with 60 μM of isolated compounds (**1**–**11**) for 24 h. (B) HeLa cells were treated with isolated compounds (**1**–**11**) in combination with ADR (1.0 μg/mL). The number of mitotic entry

cells (*white columns*) and dead cells (*red columns*) were counted using a time-lapse recording. The graph shows the percentages of mitotic entry cells and dead cells as the means ± S.D. of three independent experiments. More than 24 cells were analyzed in each experiment. Statistical significance was analyzed using the Tukey-Kramer test (*$p < 0.05$ compared with ADR at a concentration of 1.0 μg/mL).

Among the anti-cancer drugs, ADR has been used for cancer therapy for a long time. ADR inhibits cell proliferation through the induction of G2/M cell cycle arrest via DNA damage. The expression of the drug efflux transporter P-gp,[22] anti-apoptotic functions of heat shock protein (HSP),[23] and activation of detoxifying enzymes[24] were known to decrease the sensitivity to ADR on cancer cells. Therefore, inhibitors of P-gp, HSP, and detoxifying enzymes can prevent side effects by reducing ADR dosage needed in tumor therapy. Previously, we reported that the inhibitors of P-gp and HSP enhance the cytotoxicity of ADR.[8,25,26] We further evaluated the effects of isolated compounds (**1**−**11**) on the cytotoxicity of ADR using time-lapse cell imaging analysis on HeLa cells. In this study, we counted the number of mitotic entry cells and dead cells treated with ADR (0.5, 1.0, or 2.0 μg/mL), isolated compounds (**1**−**11**, 60 μM), and isolated compounds with ADR (1.0 μg/mL). The isolated compounds (**1**−**11**) did not affect the number of mitotic entry cells and dead cells (Figure 3A). On the other hand, the number of dead cells induced by ADR was increased in combination with phenolic diglycosides (**7**−**10**). Among these compounds, the number of dead cells with combination treatment of seguinoside K (**7**) and ADR was significantly larger than that of ADR-treated cells (**7** and ADR: 75.8 ± 1.7%, ADR: 41.9 ± 2.2%) (Figure 3B). Several compounds, such as topoisomerase-I inhibitor,[27] P-gp inhibitor,[28] and HSP90 inhibitor,[29] were reported to present the synergistic effect of ADR. These compounds showed cytotoxicity without ADR. However, **7** enhanced the cytotoxic effect of ADR at a nontoxic concentration. Therefore, **7** may be a potential chemotherapy enhancement agent without the side effects of cancer treatment.

EXPERIMENTAL

Specific rotations were obtained on a model P-2200 digital polarimeter (l = 5 cm; JASCO, Tokyo, Japan). UV spectra were measured on a model J-1500 spectrometer (JASCO). FTIR spectra were recorded on a model FT/IR-4600 Fourier transform infrared spectrometer (JASCO). Electrospray ionization mass spectrometry (ESIMS) and high-resolution ESIMS (HRESIMS) were recorded on a Shimadzu LCMS-IT-TOF. ^{1}H-NMR spectroscopy was recorded on JEOL ECS400 (400 MHz) and JNM-ECA 600 (600 MHz) spectrometers. ^{13}C-NMR spectroscopy was recorded on a JNM-ECA 600 (150 MHz) spectrometer. 2D-NMR experiments were conducted on a JEOL JNM-ECA 600 (600 MHz) spectrometer. Normal-phase silica gel column chromatography was performed on Silica gel 60 (Kanto Chemical, Tokyo,

Japan, 63–210 μm). Reversed-phase silica gel column chromatography was performed on C_{18}-OPN (Nacalai Tesque, Kyoto, Japan, 140 μm). HPLC was performed on SPD-M10Avp UV-vis detector (Shimadzu, Kyoto, Japan). COSMOSIL 5C18-MS-II (Nacalai Tesque, 250 × 4.6 mm i.d., 250 × 10 mm i.d. and 250 × 20 mm i.d.), COSMOSIL 5C18-AR-II (Nacalai Tesque, 250 × 4.6 mm i.d. and 250 × 10 mm i.d.), and YMC-Triart PFP (YMC, Kyoto, Japan, 250 × 4.6 mm i.d. and 250 × 10 mm i.d.) columns were used for analytical and preparative purposes.

Plant material. The fresh stems and twigs of *H. tiliaceus* were collected in the Okinawa prefecture of Japan by the Kumejimatumugi Business Cooperation (Okinawa prefecture, Japan) in February 2019.

Extraction and isolation. The fresh stems and twigs of *H. tiliaceus* (15.0 kg) were extracted three times with MeOH under reflux for 3 h. The EtOAc soluble fraction (40.1 g, 0.27%) and aqueous layer (201.5 g, 1.34%) were obtained from the MeOH extract, following the procedure described previously.[9] The aqueous layer was further extracted with *n*-BuOH to give *n*-BuOH (30.0 g, 0.20%) and water (171.6 g, 1.14%) soluble fraction. The *n*-BuOH soluble fraction was subjected to normal- and reversed-phase silica gel column chromatography [30.0 g, $CHCl_3$-MeOH–methanol (50:1 → 20:1 → 10:1 → 5:1 → 2:1, v/v) → MeOH] to give seven fractions [Fr. B1–7]. Fraction B6 (2419.7 mg) was further separated via reversed-phase silica gel column chromatography to give seven fractions [Fr. B6-1–6-7]. Fraction B6-1 (493.5 mg) was purified via HPLC {H_2O–MeCN–AcOH (85:15:0.1, v/v/v)} to give eight fractions. Fraction B6-1-1 (19.0 mg) was purified via HPLC {H_2O–MeCN (90:10, v/v)} to give **5** (7.4 mg). Fraction B6-1-2 (8.6 mg) was purified via HPLC {H_2O–MeCN (90:10, v/v)} to give **11** (2.5 mg). Fraction B6-1-4 (33.0 mg) was purified via HPLC {H_2O–MeCN (90:10, v/v)} to give **1** (2.0 mg) and **2** (7.1 mg). Fraction B6-1-5 (15.5 mg) was purified via HPLC {H_2O–MeCN (85:15, v/v)} to give **9** (2.7 mg) and **10** (1.8 mg). Fraction B6-1-7 (41.7 mg) was purified via HPLC {H_2O–MeCN (85:15, v/v)} to give **7** (10.0 mg) and **8** (5.0 mg). Fraction B6-1-8 (14.8 mg) was purified via HPLC {H_2O–MeCN (85:15, v/v)} to give **4** (5.0 mg). Fraction B6-2 (409.8 mg) was purified via HPLC {H_2O–MeCN–AcOH (80:20:0.1, v/v/v)} to give twelve fractions. Fraction B6-2-5 (24.0 mg) was purified via HPLC {H_2O–MeCN (85:15, v/v)} to give **6** (1.8 mg). Fraction B6-2-9 (48.7 mg) was purified via HPLC {H_2O–MeCN (85:15, v/v)} to give **3** (2.6 mg).

Hibiscuscoumarin (1): Colorless amorphous powder; $[\alpha]^{25}_{D}$ -65.7 (*c* 0.2, MeOH); UV (MeOH) λ_{max} (log ε) 293 (3.80), 227 (4.16), 213 (4.24) nm; IR (ATR) ν_{max} 2920, 1705, 1411, 1045 cm^{-1}; ^{1}H-NMR (CD_3OD, 600 MHz) and ^{13}C-NMR (CD_3OD, 150 MHz) see Table 1; ESIMS: *m/z* 553 $[M+Na]^+$; HRESIMS: *m/z* 553.1535 (Calcd for $C_{23}H_{30}O_{14}Na$ $[M+Na]^+$: *m/z* 553.1528).

Acid hydrolysis of hibiscuscoumarin (1). The solution of **1** (1.4 mg) in 5% aqueous H_2SO_4–1,4-dioxane (1:1) was heated at 90 ℃ for 3 h. After subjecting **1** to acid hydrolysis, solutions were neutralized and

extracted with EtOAc and water three times. After drying of the aqueous layer in vacuo, the residue was dissolved in pyridine (0.2 mL) containing L-cysteine methyl ester hydrochloride (1.0 mg), and the solution was heated at 60 ℃ for 1 h. A solution of *o*-tolyli sothiocyanate (1.0 mg) in pyridine (0.1 mL) was added, and the mixture was heated at 60 ℃ for 1 h. The mixture was analyzed by reversed-phase HPLC [column: Cosmosil 5C18-AR-II (250 × 4.6 mm i.d.), mobile phase: 18% MeCN, detection: UV (254 nm), flow rate: 1.0 mL/min, column temperature: 25 ℃] to identify the derivatives of D-glucose and L-rhamnose by comparing their retention times to those of authentic samples (D-glucose, 54.4 min; L-glucose, 50.6 min; D-rhamnose, 36.6 min; L-rhamnose, 35.3 min).

Cell culture. HeLa cells were cultured in Dulbecco's Modified Eagle's Medium with low glucose (Wako Pure Chemical Industries, Osaka, Japan) and supplemented with 5% fetal bovine serum (Sigma-Aldrich, St. Louis, MO, USA) under a 5% CO_2 atmosphere at 37 ℃.

Time-lapse imaging analysis. Time-lapse imaging was performed on an Operetta high-content imaging system (PerkinElmer, Waltham, MA, USA). HeLa cells were cultured in a flat-bottomed 96-well plate (Coster 3596; Corning, NY, USA) and incubated to reach 70−80% confluence. The cells were treated with the test compounds prior to the time-lapse cell imaging. The images were captured at 10 min intervals for 24 h under a 5% CO_2 atmosphere at 37 ℃. Based on these images, the number of mitotic cells and dead cells within 24 h was quantified.

Statistical Analysis. Statistical analyses were conducted using GraphPad Prism 8.43 software. The statistical analysis was conducted using one-way analysis of variance (ANOVA) followed by a Tukey-Kramer test to analyze the differences between the treatment groups. The differences were considered statistically significant at $*p < 0.05$.

SUPPORTING INFORMATION

Experimental details: 1D and 2D-NMR spectra for hibiscuscoumarin (**1**) are available free of charge on the Internet.

ACKNOWLEDGEMENTS

This work was supported by JSPS KAKENHI Grant Numbers 20H03397 and 20J14567.

REFERENCES

1. G. Hu, C. Hu, X. Peng, S. Lu, and Z. Zhang, *Mitochondrial DNA B Resour.*, 2021, **6**, 1904.
2. S. M. Abdul-Awal, S. Nazmir, S. Nasrin, T. R. Nurunnabi, and S. J. Uddin, *SpringerPlus*, 2016, **5**, 1209.
3. Narender, S. Kumer, D. Kumer, and V. Kumer, *Int. J. Pharmacogn. Phytochem. Res.*, 2009, **1**, 15.

4. S. Ramproshad, T. Afroz, B. Mondal, A. Haque, S. Ara, R. Khan, and S. Ahmed, *Pharmacol. Online*, 2012, **3**, 82.
5. T. Masuda, D. Yamashita, Y. Takeda, and S. Yonemori, *Biosci. Biotechnol. Biochem.*, 2005, **69**, 109.
6. T. Matsumoto, D. Imahori, Y. Saito, W. Zhang, T. Ohta, T. Yoshida, Y. Nakayama, E. Ashihara, and T. Watanabe, *J. Nat. Med.*, 2020, **74**, 689.
7. T. Matsumoto, T. Kitagawa, D. Imahori, A. Matsuzaki, Y. Saito, T. Ohta, T. Yoshida, Y. Nakayama, E. Ashihara, and T. Watanabe, *Bioorg. Med. Chem.*, 2021, **45**, 128161.
8. D. Imahori, T. Matsumoto, Y. Saito, T. Ohta, T. Yoshida, Y. Nakayama, and T. Watanabe, *Fitoterapia*, 2021, **154**, 105023.
9. T. Matsumoto, D. Imahori, K. Achiwa, Y. Saito, T. Ohta, T. Yoshida, N. Kojima, M. Yamashita, Y. Nakayama, and T. Watanabe, *Fitoterapia*, 2020, **142**, 104524.
10. R. M. Damiani, D. J. Moura, C. M. Viau, R. A. Caceres, J. A. P. Joao, and J. Saffi, *Arch. Toxicol.*, 2016, **90**, 2063.
11. S. Rivankar, *J. Cancer Res. Ther.*, 2014, **10**, 853.
12. H. Tsukamoto, S. Hisada, and S. Nishibe, *Chem. Pharm. Bull.*, 1985, **33**, 4069.
13. Z. D. He, C. Y. Ma, G. T. Tan, K. Sydara, P. Tamez, B. Southavong, S. Bouamanivong, D. D. Soejarto, J. M. Pezzuto, H. H. S. Fong, and H. J. Zhang, *Phytochemistry*, 2006, **67**, 1378.
14. N. Matsuda and M. Kikuchi, *Chem. Pharm. Bull.*, 1996, **44**, 1676.
15. K. Yoshikawa, N. Mimura, and S. Arihara, *J. Nat. Prod.*, 1998, **61**, 1137.
16. V. Dellus, I. Mila, A. Scalbert, C. Menard, V. Michon, and C. L. M. Herve Du Penhoat, *Phytochemistry*, 1997, **45**, 1573.
17. X. N. Zhong, H. Otsuka, T. Ide, E. Hirata, and Y. Takeda, *Phytochemistry*, 1999, **52**, 923.
18. M. J. Jung, S. S. Kang, Y. J. Jung, and J. S. Choi, *Chem. Pharm. Bull.*, 2004, **52**, 1501.
19. T. Yin, G. Tu, Q. Zhang, B. Wang, and Y. Zhao, *Magn. Reason. Chem.*, 2008, **46**, 387.
20. V. A. Marinos, M. E. Tate, and P. J. Williams, *Phytochemistry*, 1992, **31**, 4307.
21. T. Kitagawa, T. Matsumoto, D. Imahori, M. Kobayashi, M. Okayama, T. Ohta, T. Yoshida, and T. Watanabe, *J. Nat. Med.*, 2021, **75**, 998.
22. G. Szakács, J. K. Paterson, J. A. Ludwig, C. Booth-Genthe, and M. M. Gottesman, *Nat. Rev. Drug Discov.*, 2006, **5**, 219.
23. T. Yamane, Y. Saito, H. Teshima, M. Hagino, A. Kakihana, S. Sato, M. Shimada, Y. Kato, T. Kuga, N. Yamagishi, and Y. Nakayama, *J. Cell. Biochem.*, 2019, **120**, 17951.
24. Y. Kondo, E. S. Woo, A. E. Michalska, K. H. A. Choo, and J. S. Lazo, *Cancer Res.*, 1995, **55**, 2021.
25. T. Matsumoto, T. Kitagawa, D. Imahori, H. Yoshikawa, M. Okayama, M. Kobayashi, N. Kojima, M.

Yamashita, and T. Watanabe, *J. Nat. Med.*, 2021, **75**, 942.

26. T. Matsumoto, D. Imahori, E. Ohnishi, M. Okayama, T. Kitagawa, T. Ohta, T. Yoshida, N. Kojima, M. Yamashita, and T. Watanabe, *Fitoterapia*, 2022, **156**, 105097.
27. T. Saotome, T. Takagi, C. Sakai, K. Kumagai, and J. Tamaru, *Ann. Oncol.*, 2000, **11**, 115.
28. S. A. Khaleel, A. M. Al-Abd, A. A. Ali, and A. B. Abdel-Naim, *Sci. Rep.*, 2016, **6**, 36855.
29. H. K. Park, J. E. Lee, J. Lim, D. E. Jo, S. A. Park, P. G. Suh, and B. H. Kang, *BMC Cancer*, 2014, **14**, 431.